



Value of blood oxygenation level-dependent MRI for predicting clinical outcomes in uterine cervical cancer treated with concurrent chemoradiotherapy

Jiyeong Lee¹ · Chan Kyo Kim^{1,2} · Kyo-won Gu¹ · Won Park³

Received: 8 February 2019 / Revised: 15 March 2019 / Accepted: 25 March 2019 / Published online: 23 April 2019
© European Society of Radiology 2019

Abstract

Objectives To investigate the value of blood oxygenation level-dependent (BOLD) MRI as a predictor of clinical outcomes in cervical cancer patients treated with concurrent chemoradiotherapy (CCRT).

Method Enrolled 92 patients with stage IB2–IVB cervical cancer who received CCRT underwent 3-T BOLD MRI before treatment. The R2* value (rate of spin dephasing, s⁻¹) was measured in the tumor. Cox regression analysis was used to evaluate the associations of imaging and clinical parameters with progression-free survival (PFS) and cancer-specific survival (CSS). Inter-reader reliability for the R2* measurements was evaluated using an intraclass correlation coefficient (ICC).

Results Tumor R2* values were significantly different between patients with and without disease progression ($p < 0.001$). Multivariate analysis demonstrated that tumor R2* value was significantly independent factor for PFS (hazard ratio [HR] = 5.746, $p < 0.001$) and CSS (HR = 12.878, $p = 0.001$). Additionally, squamous cell carcinoma antigen (HR = 1.027, $p = 0.001$) was significantly independent factor for PFS. Inter-reader reliability for the R2* measurements was good (ICC = 0.702).

Conclusion Pretreatment 3-T BOLD MRI may be useful for predicting clinical outcomes in uterine cervical cancer patients treated with CCRT, with good inter-reader reliability.

Key Points

- Tumor R2* values are different between patients with and without disease progression.
- The R2* value is an independent factor for treatment outcomes in cervical cancer.
- Inter-reader reliability for R2* measurements using BOLD MRI is good.

Keywords Cervical cancer · Magnetic resonance imaging · Radiotherapy · Hypoxia · Treatment outcome

Abbreviations

BOLD Blood oxygenation level-dependent
CCRT Concurrent chemoradiotherapy

CI Confidence interval
CSS Cancer-specific survival
EBRT External beam radiotherapy
FIGO International Federation of Gynecology and Obstetrics
HR Hazard ratio
ICC Intraclass correlation coefficient
LN Lymph node
MRI Magnetic resonance imaging
OS Overall survival
PFS Progression-free survival

Chan Kyo Kim and Won Park contributed equally to this work.

✉ Chan Kyo Kim
chankyokim@skku.edu

¹ Department of Radiology and Center for Imaging Science, Samsung Medical Center, Sungkyunkwan University School of Medicine, 81 Irwon-Ro, Gangnam-gu, Seoul 06351, Republic of Korea

² Department of Medical Device Management & Research, SAIHST, Sungkyunkwan University, Seoul, Republic of Korea

³ Department of Radiation Oncology, Samsung Medical Center, Sungkyunkwan University School of Medicine, Seoul, Republic of Korea

Introduction

Concurrent chemoradiotherapy (CCRT) is the standard treatment of locally advanced cervical cancer for the International

Federation of Gynecology and Obstetrics (FIGO) stage IB2–IVA [1]. However, a substantial number of patients experience locoregional recurrence or distant metastasis after treatment [2]. Thus, predicting clinical outcomes, such as disease progression or survival during or early after treatment, is important for improving patient treatment and counseling.

Hypoxic cervical cancers are associated with poor clinical outcomes, regardless of treatment modality, which is independent of standard prognostic factors, such as depth of tumor invasion and lymph node (LN) metastasis [3]. Detection of tumor hypoxia has been performed using invasive polarographic needle electrodes [4], but noninvasive imaging techniques, such as dynamic contrast-enhanced magnetic resonance imaging (DCE-MRI), diffusion-weighted imaging, CT, or blood oxygenation level-dependent (BOLD) MRI, have recently provided promising results for predicting the therapeutic response of cervical cancer [5–10].

The BOLD MRI technique uses the slight increase in T2* signals from paramagnetic deoxyhemoglobin to quantify the oxygenation status of the tumor immediately adjacent to perfused microvessels [11]. Recent studies have reported that BOLD MRI is feasible for evaluating cervical cancer [12–14] and is a reproducible technique for assessing early therapeutic changes to CCRT [15]. Based on the results of these studies, we hypothesized that the degree of tumor oxygenation measured using pretreatment BOLD MRI might be useful for predicting treatment outcomes in patients with cervical cancer undergoing CCRT. To the best of knowledge, no studies have investigated the utility of BOLD MRI in predicting clinical outcomes in cervical cancer, with mid-term or long-term follow-up. Therefore, the present study aimed to evaluate the value of pretreatment BOLD MRI in predicting clinical outcomes in patients with cervical cancer treated with CCRT.

Materials and methods

Patients

This study's retrospective protocol was approved by our institutional review board and waived the need for informed consent. Between October 2009 and September 2015, 97 biopsy-proven cervical cancer patients received CCRT at our institution and also underwent pretreatment MRI. The inclusion criteria were as follows: (1) the patients had biopsy-proven cervical cancer before treatment, (2) the patients had undergone 3-T BOLD MRI at our institution before treatment, and (3) the patients had not previously undergone surgery, radiotherapy, or chemotherapy. Of these, 5 patients were excluded due to severe artifacts. Thus, 92 consecutive patients treated with CCRT were included in this study.

MRI

All patients underwent pretreatment pelvic MRI that was performed using a 3-T MR scanner (Intera Achieva 3.0 TX; Philips Medical System, Best, The Netherlands) with a phased-array body coil. The routine MR sequences were T1-weighted, T2-weighted, and DCE-MRI. In addition to the routine protocols, BOLD MRI was obtained before the administration of contrast materials using a multiple fast field echo sequence to acquire 12 T2*-weighted images in the sagittal plane. The parameters were as follows: TR, 260 ms; range of echo time (TE), 5–60 ms; flip angle, 27°; slice thickness, 5 mm; interslice gap, 1 mm. The 12 T2*-weighted images corresponding to 12 different gradient echoes were obtained for each section during a single 32.5-s breath-hold.

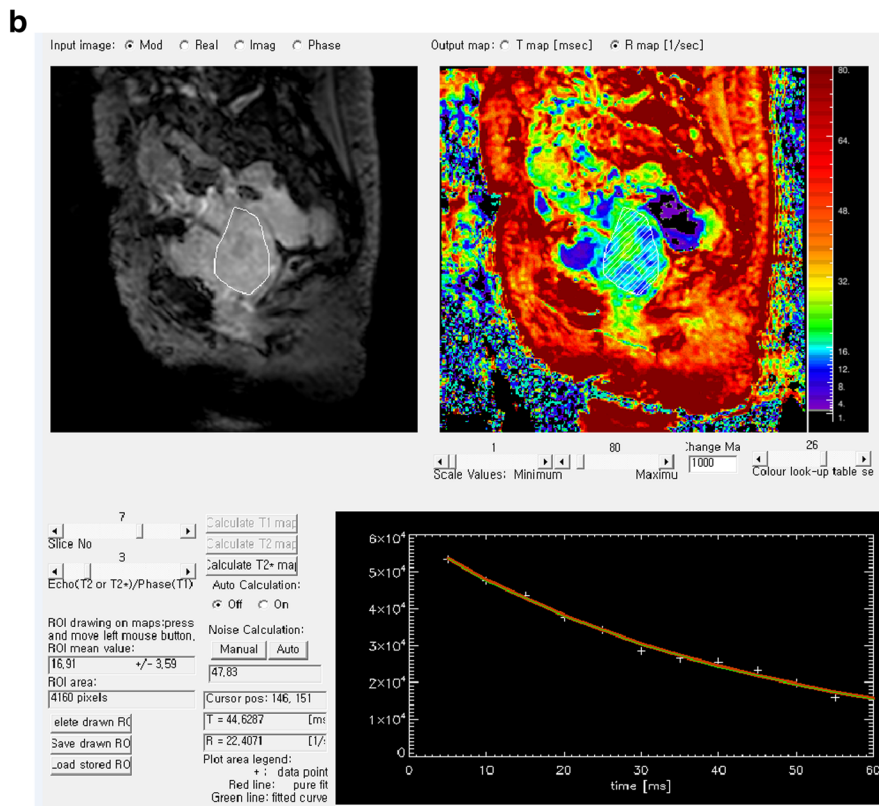
Image analysis

All images were analyzed by a genitourinary radiologist (C.K.K., with 13 years of experience in gynecological MRI). The radiologist was blinded to the clinical and pathologic results of each patient but was aware that the patients had received CCRT for biopsy-proven cervical cancer. Regarding each cervical cancer evaluated, tumor size, parametrial invasion status at MRI, LN metastasis, histology, FIGO stage, squamous cell carcinoma (SCC) antigen, and distant metastasis were recorded. The definition of LN metastasis in the abdomen and pelvis was ≥ 1 cm short-axis diameter on MRI findings [16].

After data acquisition, all images were transferred to an independent workstation for analysis with manufacturer-supplied software (PRIDE, version 4.2, Philips Healthcare). This program generates a set of color-coded parametric images of R2* (s^{-1}) from a voxel basis to an exponential function, which describes the expected signal decay as a function of TE and solving for the unknown value of R2*. On the map, red indicates the highest R2* levels and reflects a high concentration of deoxyhemoglobin, while blue indicates the lowest R2* levels and reflects a low concentration of deoxyhemoglobin.

On the color-coded R2* maps, the R2* values in the tumor were calculated using manual placement of a region of interest (ROI) by an experienced radiologist (C.K.K.). The ROI was drawn manually based on the findings of T2-weighted and dynamic contrast-enhanced imaging and encompassed as

Fig. 1 Method of R2* value measurement on color-coded R2* maps using manual placement of region of interest (ROI), based on the findings of T2-weighted imaging. **(a)** Sagittal T2-weighted image shows a large stage IVA cervical cancer with invasion to urinary bladder (arrow). **(b)** The ROI is seen on sagittal T2*-weighted image (upper left) and sagittal color-coded R2* map (upper right). The mean R2* value in cervical cancer is $16.91 s^{-1}$. The right lower image demonstrates the expected signal decay as a function of echo time



much of the tumor as possible in an image that had the greatest visibility, while avoiding adjacent structures (Fig. 1). An average of three measurements was obtained for each tumor. The mean number of pixels covering the tumor was 447 (range, 140–1565). To evaluate interobserver agreement, a less-experienced radiologist (J.L., with 2 years of experience in gynecological MRI) independently measured the tumor R2* values for all patients using the same method as the experienced radiologist. These measurements were performed on different days.

Treatment protocol

The patients underwent CCRT, which involved three-dimensional conformal external beam radiotherapy (EBRT) and 18F-fluorodeoxyglucose positron emission tomography/CT or CT-guided brachytherapy with midline shielding. The EBRT was delivered using 10- or 15-MV photons at a median dose of 50.4 Gy (range, 40–66.4 Gy) in daily fractions of 1.8–2.0 Gy over 6 weeks. High-dose intracavitary brachytherapy with an iridium-192 source was performed to deliver a total dose of 24 Gy, with 4 Gy per insertion three times per week in six fractions using a tandem and two ovoids. The EBRT was accompanied by concurrent chemotherapy that involved six cycles of weekly cisplatin (30 mg/mm²) for 59 patients or three cycles of 5-fluorouracil (1.000 mg/m²) plus cisplatin (60 mg/m²) at 3-week intervals for 33 patients. The median overall treatment time was 53.5 days (range, 43–59 days). The selection of chemotherapeutic regimen was individualized according to the extent of the local tumor, LN involvement, and the patient's general health.

Treatment outcomes

All patients were followed with clinical and radiological examinations approximately every 3 months for the first 2 years, every 6 months for the next 3 years, and then annually thereafter. Physical examinations, Pap smears, and serum tumor markers were also evaluated. Follow-up abdominopelvic MRI or CT and chest radiography were routinely performed during the annual follow-up. Disease progression was categorized as local-regional recurrence or distant metastasis. Local recurrence was considered as the presence of histologically confirmed or definite progressive disease at the cervix, vagina, or parametrium during the follow-up period. Regional recurrence was considered to occur at a pelvic LN or pelvic sidewall. Distant metastasis was considered to occur at a retroperitoneal LN and/or other organ.

Statistical analysis

Groups of patients with and without disease progression were compared to identify differences in age, tumor size,

parametrial invasion, LN metastasis, tumor marker, histology, and R2* using the independent *t* test, Fisher's exact test, Wilcoxon rank sum test, or chi-square tests. The mean R2* values obtained by the two radiologists were used for statistical analysis.

Survival outcomes were progression-free survival (PFS) and cancer-specific survival (CSS), which were all calculated from the start of treatment. Univariate and multivariate Cox regression analyses were used to determine whether the clinical and imaging parameters were associated with survival outcomes. Parameters that had univariate *p* values of < 0.25 were included in the multivariate analysis. The *p* values and 95% confidence intervals (CIs) for the hazard ratios (HRs) were corrected using Bonferroni's method. Similar analyses were performed including the optimal cutoff value of R2* which was determined at the point which the log-rank *p* value is at minimum [17]. Kaplan-Meier curves were compared using the log-rank test. The R2* values of patients with and without disease progression and cancer-specific death were compared using the independent *t* test or Wilcoxon rank sum test. Inter-reader reliability and variability were evaluated using the intraclass correlation coefficient (ICC) and the coefficient of variation (CV), respectively. The ICC value was determined to provide a reliability that was poor (0.00–0.20), fair (0.21–0.40), moderate (0.41–0.60), good (0.61–0.80), or excellent (0.81–1.00). A two-sided *p* value of < 0.05 was considered statistically significant for all analyses, which were performed using SAS software (version 9.4; SAS Institute) and R software (R 3.3.2; <https://www.R-project.org>).

Results

Baseline characteristics

The patients' characteristics are summarized in Table 1. The group with disease progression had significantly greater tumor size than that without progression (*p* = 0.031). The mean tumor R2* values of patients with progression (23.3) and cancer-specific death (24.4) were significantly greater than in those without progression (19.9) and cancer-specific death (20.6) (*p* < 0.001 and *p* < 0.001, respectively) (Fig. 2). The FIGO stage was also significantly different between the two groups (*p* < 0.001), and the group with progression had a significantly higher rate of LN metastasis than that without progression (*p* < 0.001). There were no other significant differences between the two groups (all *p* > 0.05).

Survival

During a median follow-up period of 45.5 months (range, 2.7–83.8 months), 13 (13.3%) patients died of their disease. Disease progression was identified in 32 (34.8%) patients:

Table 1 Patient characteristics

Variable	Progression (-)	Progression (+)	<i>p</i> value
Number of patient	60 (65.2)	32 (34.8)	
Age (year)	55.30 ± 11.39	56.16 ± 10.85	0.724
Size (cm)	5.3 ± 1.6	6.3 ± 2.3	0.031
LN metastasis			< 0.001
Present	18 (30.0)	23 (71.9)	
Absent	42 (70.0)	9 (28.1)	
Parametrial invasion			0.734
Present	54 (90.0)	28 (87.5)	
Absent	6 (10.0)	4 (12.5)	
R2* (s ⁻¹)	19.9 ± 2.5	23.3 ± 4.0	< 0.001
SCC antigen (ng/ml)	9.83 ± 14.18	17.31 ± 27.14	0.153
Histology			0.090
SCC	53 (88.3)	23 (71.9)	
Adenocarcinoma/other	7 (11.7)	9 (28.1)	
FIGO			< 0.001
IB2	0 (0.0)	1 (3.1)	
IIA	11 (18.3)	3 (9.4)	
IIB	36 (60.0)	11 (34.4)	
IIIA	3 (5.0)	4 (12.5)	
IIIB	1 (1.7)	11 (34.4)	
IVA	4 (6.7)	2 (6.2)	
IVB	5 (8.3)	0 (0.0)	
Progression type			
Local-regional		12 (37.5)	
Distant metastasis		15 (46.9)	
Both		5 (15.6)	

Data are mean ± standard deviation or *n* (%)

locoregional recurrence (*n* = 12), distant metastasis (*n* = 15), or both (*n* = 5). Among the 12 patients with locoregional recurrence, 10 had a recurrent tumor in the uterine cervix, 1 had regional metastatic LNs in the pelvis, and 1 had recurrent tumors in both the uterine cervix and pelvic LNs. In 21 patients, distant metastasis beyond the pelvis was found in the lung, liver, brain, and bone and multiple LNs in the supraclavicular, mediastinal, para-aortic, and axillary areas.

The 3-year and 4-year PFS rates were 67% (95% CI, 58–78%) and 66% (95% CI, 56–77%), respectively. The 3-year and 4-year CSS rates were 86% (95% CI, 78–94%) and 84% (95% CI, 76–93%), respectively.

Risk factors associated with treatment outcome

Tables 2 and 3 present the results of the Cox regression analyses for PFS and CSS. The optimal R2* cutoff values were 22.9 s⁻¹ for PFS and 22.1 s⁻¹ for CSS. Univariate analysis demonstrated that tumor size, LN metastasis, SCC antigen,

histology, FIGO stage, and R2* value were significantly associated with PFS (all *p* < 0.05). However, multivariate analysis revealed that R2* value (> 22.9 s⁻¹) (HR = 5.746, *p* < 0.001) and SCC antigen (HR = 1.027, *p* = 0.001) were significant independent predictors. For predicting CSS, R2* value (> 22.1 s⁻¹), LN metastasis, and FIGO stage were significantly associated factors on univariate analysis (all *p* < 0.05). However, R2* value was the only independent predictor (HR = 12.878, *p* = 0.001) on multivariate analysis.

The actuarial PFS was worse in patients with R2* > 22.9 s⁻¹ than in those with R2* ≤ 22.9 s⁻¹, with 3-year and 4-year rates of 27% (95% CI, 14–52%) and 22% (95% CI, 11–48%), respectively, compared with 83% (95% CI, 74–93%) and 83% (95% CI, 74–93%) (*p* < 0.001) (Fig. 3). Patients with R2* > 22.1 s⁻¹ had a worse outcome than those with R2* ≤ 22.1 s⁻¹, with 3-year and 4-year CSS rates of 61% (95% CI, 44–84%) and 55% (95% CI, 38–80%) compared with 97% (95% CI, 92–100%) and 97% (95% CI, 92–100%) (*p* < 0.001), respectively (Fig. 3).

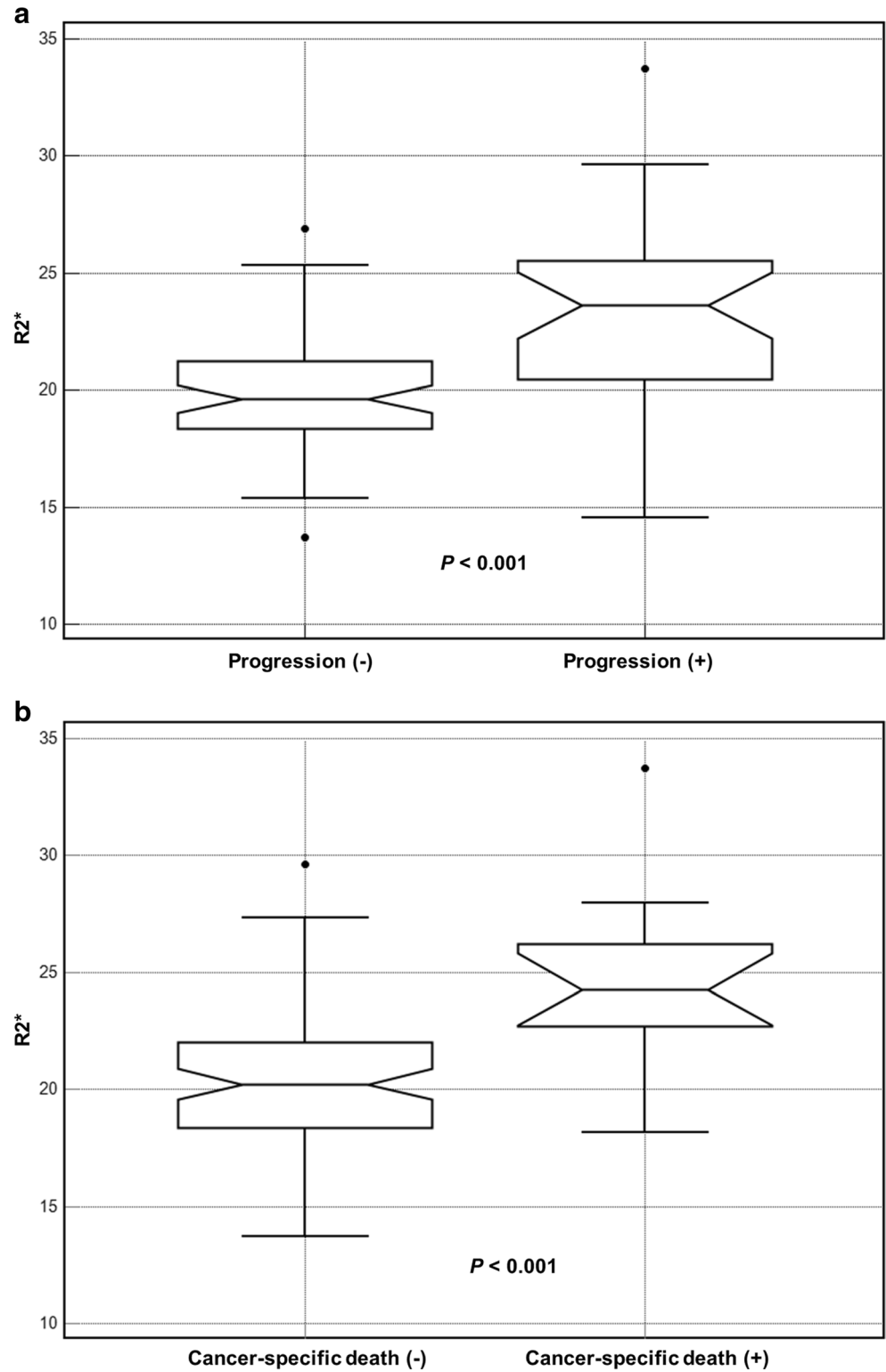
Inter-reader reliability and variability

For the inter-reader reliability and variability of the R2* measurements, ICC and CV were 0.702 (95% CI, 0.521–0.858) and 12.2%, respectively.

Discussion

Tumor hypoxia affects therapeutic response through increased resistance to radiation and expression of genes encoding for metastasis-promoting proteins, although the resistance to some cytotoxic agents may decrease [18, 19]. In addition, tumor hypoxia can induce the development of an aggressive phenotype that is caused by restrained proliferation, differentiation, necrosis, or apoptosis [20]. In cervical cancer, hypoxia is associated with poorer outcomes and is an independent predictor for metastasis and survival [21, 22]. Thus, stratifying cervical cancer patients based on pretreatment hypoxia may allow the physician to tailor the treatment strategy to the characteristics of the tumor, which may improve the success opportunities of personalized treatment. The present study involved a mid-term follow-up (median, 45.5 months) of 92 patients treated with CCRT, and demonstrated that the pretreatment R2* value of cervical cancer was the only independent factor for disease progression and survival. Furthermore, patients with R2* greater than the cutoff values demonstrated significantly worse PFS and CSS than those with lower than the cutoff values. Thus, these findings indicate that pretreatment tumor R2* value may be a useful prognostic marker for treatment outcome in cervical cancer patients undergoing CCRT, which may allow physicians to better counsel and select optimal adjuvant treatment.

Fig. 2 Box-whisker plots demonstrate R2* values of patients with and without progression (a) and cancer-specific death (b). Central horizontal line = mean, and box = 25% and 75% confidence intervals



The BOLD MRI technique indirectly measures blood oxygenation using the R2* parameter (i.e., rate of spin dephasing = 1 / T2* relaxation time), which is based on the fact that deoxyhemoglobin is paramagnetic while oxyhemoglobin is not [23]. Thus, a high deoxyhemoglobin concentration will cause a reduction in the T2* relaxation time of the protons and

dephasing of the surrounding tissues. Therefore, high R2* values indicate a high proportion of deoxyhemoglobin and a relatively low level of blood oxygenation [24]. Furthermore, BOLD MRI can be repeated without the administration of an exogenous contrast agent, which may allow for its routine use in clinical practice as a noninvasive imaging technique.

Table 2 Cox regression analysis of clinical and MRI variables for PFS

Variable	Univariate			Multivariate		
	HR	95% CI	<i>p</i> value	HR	95% CI	<i>p</i> value
Age	1.010	0.979–1.042	0.536			
Tumor size	1.021	1.005–1.037	0.010	0.998	0.976–1.020	0.864
LN metastasis	4.008	1.852–8.671	<0.001	2.125	0.892–5.065	0.089
Parametrial invasion	0.883	0.310–2.518	0.816			
SCC antigen	1.016	1.001–1.030	0.036	1.027	1.011–1.044	0.001
Histology	2.494	1.146–5.429	0.021	2.335	0.869–6.276	0.093
FIGO (\geq IIB)	2.956	1.472–5.936	0.002	1.260	0.574–2.768	0.565
R2* ($>$ 22.9)	6.860	3.311–14.210	<0.001	5.746	2.390–13.814	<0.001

Only a few preliminary studies have investigated the utility of BOLD MRI for evaluating oxygenation in cervical cancer [12–15]. For example, O'Connor et al [12] used BOLD MRI to monitor changes in oxygenation in 10 solid tumors by measuring changes in the longitudinal relaxation rates with patients breathing atmospheric air (21% oxygen) and then breathing 100% oxygen. However, that study only included 2 patients with cervical cancer. Hallac et al [14] also reported that 3-T BOLD MRI was a feasible tool for evaluating 10 patients with cervical cancer. Two recent studies [13, 15] have also demonstrated that BOLD MRI could predict the therapeutic response of cervical cancer to CCRT. In their studies, tumor R2* had a significantly negative correlation with the percentage of tumor shrinkage in 30 patients [13] and may demonstrate early physiologic changes to CCRT in 15 patients with cervical cancers [15]. Until now, to the best of our knowledge, no studies have published the utility of BOLD MRI in cervical cancer for predicting treatment outcome. Our results demonstrated that BOLD MRI may be a useful technique for predicting treatment outcome in patients with cervical cancer after CCRT.

Interestingly, a previous study [25] of 40 patients with uterine cervical cancer investigated whether one of the parameters was more important for disease control than the others. In their study, tumor oxygen tension was measured polarographically before and after 2 weeks of RT. They found that pretreatment

oxygenation is more important for disease control than the oxygenation after 2 weeks of RT or changes in oxygenation during this time. Our results demonstrated that pretreatment R2* value of cervical cancer was a significant independent predictor of progression and survival on multivariate analysis. Moreover, with an optimal cutoff value of R2* (22.9 s⁻¹ for PFS and 22.1 s⁻¹ for CSS), patients with a greater than optimal cutoff value had significantly worse progression and survival than those with optimal cutoff value or less. However, further studies will be needed because these cutoff values on BOLD MRI might be affected by several parameters.

It is clear that if quantitative parameters are to be used as tools to evaluate tumor response, assessing inter-reader or intra-reader agreement or variability is a prerequisite. In our study of R2* measurements, interobserver reliability was good and interobserver variability was 12.2%. Therefore, we believe that the R2* measurement in cervical cancer might be a reliable tool to predict treatment outcome after CCRT.

Many previous studies have reported that various variables such as age, FIGO, tumor size, SCC antigen, or histology are prognostic markers for treatment outcome [26–28]. In our study, SCC antigen was the independent predictor for PFS on multivariate analysis. These results were in line with those of previous studies that elevated SCC antigen before treatment was associated with poor survival during follow-up period [28].

Table 3 Cox regression analysis of clinical and MRI variables for CSS

Variable	Univariate			Multivariate		
	HR	95% CI	<i>p</i> value	HR	95% CI	<i>p</i> value
Age	1.031	0.983–1.082	0.212			
Tumor size	1.010	0.981–1.039	0.512			
LN metastasis	3.341	1.029–10.852	0.045	1.964	0.583–6.618	0.276
Parametrial invasion	0.683	0.151–3.081	0.619			
SCC antigen	1.009	0.987–1.030	0.434			
Histology	1.957	0.532–7.201	0.313			
FIGO (\geq IIB)	0.127	0.016–0.990	0.049	0.523	0.064–4.292	0.546
R2* ($>$ 22.1)	15.490	3.421–70.170	<0.001	12.878	2.2762–60.036	0.001

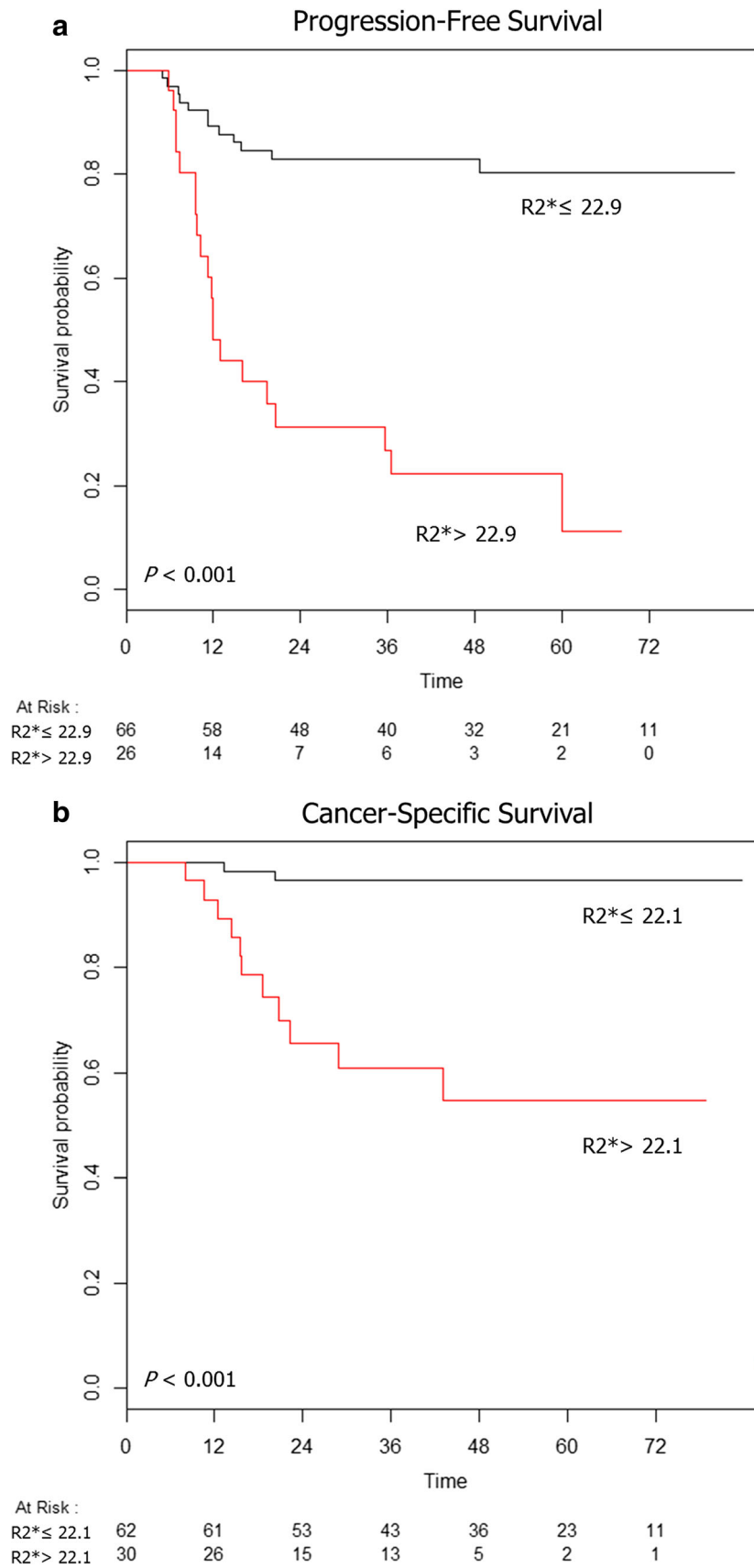


Fig. 3 Kaplan-Meier analyses of PFS (a) and CSS (b) of patients with < cutoff value of $R2^*$ versus \geq cutoff value of $R2^*$. Cutoff values of $R2^*$ are 22.9 s^{-1} for PFS and 22.1 s^{-1} for CSS, respectively

There were several limitations to our study. First, we could not evaluate the correlation between BOLD effects and histopathological findings because we did not obtain surgical specimens. A detailed correlation between BOLD MRI and histopathological findings should be determined in the future using a preclinical animal study. Second, the mean $R2^*$ change within the ROI of the tumor has limited utility in evaluating therapeutic response with regard to the heterogeneity of the tumor. Thus, histogram analyses may improve the estimation of tumor heterogeneity. Third, the patient population was relatively small. Although the follow-up period of our study was mid-term of median 45.5 months, a validation of BOLD MRI as a prognostic factor is awaited during the long-term follow-up period. Fourth, $R2^*$ value may reflect blood oxygenation in the tumor. However, in addition to oxygenation, $R2^*$ value is affected by other factors, such as blood flow, hemoglobin level, blood volume, and vasculature. The relationship between this change in $R2^*$ and tumor oxygenation physiology is unclear. Therefore, further studies involving pathophysiologic and hemodynamic analyses are needed. Finally, only a radiologist assessed all MRI findings, except $R2^*$ measurement in the tumor.

In conclusion, our results demonstrated that pretreatment BOLD MRI as a prognostic marker may be useful for predicting clinical outcome in patients with cervical cancer treated with CCRT, with good inter-reader reliability.

Funding This study was supported by Basic Science Research Program through the National Research Foundation of Korea (NRF) funded by the Ministry of Education (NRF-2017R1A2B4006020).

Compliance with ethical standards

Guarantor The scientific guarantor of this publication is Chan Kyo Kim.

Conflict of interest The authors of this manuscript declare no relationships with any companies whose products or services may be related to the subject matter of the article.

Statistics and biometry Insuk Sohn, PhD, of Statistics and Data Center, Samsung Medical Center, kindly provided statistical advice for this manuscript.

Informed consent This retrospective study was approved by our institutional review board, with a waiver of the requirement for informed consent.

Ethical approval Institutional Review Board approval was obtained.

Methodology

- Retrospective
- Diagnostic or prognostic study
- Performed at one institution

References

1. Datta NR, Stutz E, Liu M et al (2017) Concurrent chemoradiotherapy vs. radiotherapy alone in locally advanced cervix cancer: a systematic review and meta-analysis. *Gynecol Oncol* 145:374–385
2. Rose PG, Bundy BN, Watkins EB et al (1999) Concurrent cisplatin-based radiotherapy and chemotherapy for locally advanced cervical cancer. *N Engl J Med* 340:1144–1153
3. Fyles A, Milosevic M, Hedley D et al (2002) Tumor hypoxia has independent predictor impact only in patients with node-negative cervix cancer. *J Clin Oncol* 20:680–687
4. Bentzen L, Keiding S, Nordmark M et al (2003) Tumour oxygenation assessed by ^{18}F -fluoromisonidazole PET and polarographic needle electrodes in human soft tissue tumours. *Radiother Oncol* 67:339–344
5. Mannelli L, Patterson AJ, Zahra M et al (2010) Evaluation of nonenhancing tumor fraction assessed by dynamic contrast-enhanced MRI subtraction as a predictor of decrease in tumor volume in response to chemoradiotherapy in advanced cervical cancer. *AJR Am J Roentgenol* 195:524–527
6. Mayr NA, Yuh WT, Zheng J et al (1998) Prediction of tumor control in patients with cervical cancer: analysis of combined volume and dynamic enhancement pattern by MR imaging. *AJR Am J Roentgenol* 170:177–182
7. Zahra MA, Tan LT, Priest AN et al (2009) Semiquantitative and quantitative dynamic contrast-enhanced magnetic resonance imaging measurements predict radiation response in cervix cancer. *Int J Radiat Oncol Biol Phys* 74:766–773
8. Gui B, Micco M, Valentini AL et al (2018) Prospective multimodal imaging assessment of locally advanced cervical cancer patients administered by chemoradiation followed by radical surgery—the “PRICE” study 2: role of conventional and DW-MRI. *Eur Radiol*
9. Thomeer MG, Vandecaveye V, Braun L et al (2019) Evaluation of T2-W MR imaging and diffusion-weighted imaging for the early post-treatment local response assessment of patients treated conservatively for cervical cancer: a multicentre study. *Eur Radiol* 29:309–318
10. Yang W, Qiang JW, Tian HP, Chen B, Wang AJ, Zhao JG (2018) Multi-parametric MRI in cervical cancer: early prediction of response to concurrent chemoradiotherapy in combination with clinical prognostic factors. *Eur Radiol* 28:437–445
11. Wakefield JC, Downey K, Kyriazi S, deSouza NM (2013) New MR techniques in gynecologic cancer. *AJR Am J Roentgenol* 200:249–260
12. O'Connor JP, Naish JH, Parker GJ et al (2009) Preliminary study of oxygen-enhanced longitudinal relaxation in MRI: a potential novel biomarker of oxygenation changes in solid tumors. *Int J Radiat Oncol Biol Phys* 75:1209–1215
13. Kim CK, Park SY, Park BK, Park W, Huh SJ (2014) Blood oxygenation level-dependent MR imaging as a predictor of therapeutic response to concurrent chemoradiotherapy in cervical cancer: a preliminary experience. *Eur Radiol* 24:1514–1520
14. Hallac RR, Ding Y, Yuan Q et al (2012) Oxygenation in cervical cancer and normal uterine cervix assessed using blood oxygenation level-dependent (BOLD) MRI at 3T. *NMR Biomed* 25:1321–1330
15. Choi SH, Kim CK, Park JJ, Park BK (2016) Assessment of early therapeutic changes to concurrent chemoradiotherapy in uterine cervical cancer using blood oxygenation level-dependent magnetic resonance imaging. *J Comput Assist Tomogr* 40:730–734
16. Sironi S, Buda A, Picchio M et al (2006) Lymph node metastasis in patients with clinical early-stage cervical cancer: detection with integrated FDG PET/CT. *Radiology* 238:272–279

17. Budczies J, Klauschen F, Sinn BV et al (2012) Cutoff Finder: a comprehensive and straightforward web application enabling rapid biomarker cutoff optimization. *PLoS One* 7:e51862
18. Adams GE, Hasan NM, Joiner MC (1997) The Klaas Breur Lecture. Radiation, hypoxia and genetic stimulation: implications for future therapies. *Radiother Oncol* 44:101–109
19. Brown JM, Giaccia AJ (1998) The unique physiology of solid tumors: opportunities (and problems) for cancer therapy. *Cancer Res* 58:1408–1416
20. Lyng H, Sundfor K, Trope C, Rofstad EK (2000) Disease control of uterine cervical cancer: relationships to tumor oxygen tension, vascular density, cell density, and frequency of mitosis and apoptosis measured before treatment and during radiotherapy. *Clin Cancer Res* 6:1104–1112
21. Lyng H, Malinen E (2017) Hypoxia in cervical cancer: from biology to imaging. *Clin Transl Imaging* 5:373–388
22. Pacheco-Torres J, Lopez-Larrubia P, Ballesteros P, Cerdan S (2011) Imaging tumor hypoxia by magnetic resonance methods. *NMR Biomed* 24:1–16
23. Price JM, Robinson SP, Koh DM (2013) Imaging hypoxia in tumours with advanced MRI. *Q J Nucl Med Mol Imaging* 57:257–270
24. Li SP, Padhani AR, Makris A (2011) Dynamic contrast-enhanced magnetic resonance imaging and blood oxygenation level-dependent magnetic resonance imaging for the assessment of changes in tumor biology with treatment. *J Natl Cancer Inst Monogr* 2011:103–107
25. Li XS, Fan HX, Fang H, Song YL, Zhou CW (2015) Value of R2* obtained from T2*-weighted imaging in predicting the prognosis of advanced cervical squamous carcinoma treated with concurrent chemoradiotherapy. *J Magn Reson Imaging* 42:681–688
26. Sturdza A, Potter R, Fokdal LU et al (2016) Image guided brachytherapy in locally advanced cervical cancer: improved pelvic control and survival in RetroEMBRACE, a multicenter cohort study. *Radiother Oncol* 120:428–433
27. Moore KN, Java JJ, Slaughter KN et al (2016) Is age a prognostic biomarker for survival among women with locally advanced cervical cancer treated with chemoradiation? An NRG Oncology/Gynecologic Oncology Group ancillary data analysis. *Gynecol Oncol* 143:294–301
28. Hirakawa M, Nagai Y, Inamine M et al (2008) Predictive factor of distant recurrence in locally advanced squamous cell carcinoma of the cervix treated with concurrent chemoradiotherapy. *Gynecol Oncol* 108:126–129

Publisher's note Springer Nature remains neutral with regard to jurisdictional claims in published maps and institutional affiliations.